Cellular Physiology and Biochemistry

Cell Physiol Biochem 2018;46:713-726
DOI: 10.1159/000488727
Published online: April 05, 2018
Accepted: January 16, 2018

Original Paper

Carnosine Catalyzes the Formation of the Oligo/Polymeric Products of Methylglyoxal

Tim Weigand[a] Benjamin Singler[a] Thomas Fleming[b] Peter Nawroth[b,c,d] Karel D. Klika[e] Christian Thiel[a] Hans Baelde[f] Sven F. Garbade[a] Andreas H. Wagner[g] Markus Hecker[g] Benito A. Yard[h] Albert Amberger[i] Johannes Zschocke[i] Claus P. Schmitt[a] Verena Peters[a]

[a]Centre for Paediatric and Adolescent Medicine, University Hospital of Heidelberg, Heidelberg, [b]Department of Medicine I and Clinical Chemistry, University Hospital of Heidelberg, Heidelberg, [c]German Center for Diabetes Research (DZD), Neuherberg, [d]Institute for Diabetes and Cancer IDC Helmholtz Center Munich, Germany & Joint Heidelberg-IDC Translational Diabetes Program, Neuherberg, [e]Core Facility, Molecular Structure Analysis, German Cancer Research Center (DKFZ), Heidelberg Germany; [f]Department of Pathology, Leiden University Medical Center, Leiden, The Netherlands; [g]Department of Cardiovascular Physiology, Heidelberg University, [h]Department of Nephrology, Endocrinology and Rheumatology, Fifth Department of Medicine, Medical Faculty Mannheim of the University of Heidelberg, Mannheim, Germany; [i]Division of Human Genetics, Medical University Innsbruck, Innsbruck, Austria

Key Words
Diabetic nephropathy • Carnosine • Anserine • Methylglyoxal • Renal cells • Taurine transporter

Abstract
Background/Aims: Reactive dicarbonyl compounds, such as methylglyoxal (MG), contribute to diabetic complications. MG-scavenging capacities of carnosine and anserine, which have been shown to mitigate diabetic nephropathy, were evaluated *in vitro* and *in vivo*. ***Methods:*** MG-induced cell toxicity was characterized by MTT and MG-H1-formation, scavenging abilities by Western Blot and NMR spectroscopies, cellular carnosine transport by qPCR and microplate luminescence and carnosine concentration by HPLC. ***Results:*** *In vitro*, carnosine and anserine dose-dependently reduced *N*-carboxyethyl lysine (CEL) and advanced glycation end products (AGEs) formation. NMR studies revealed the formation of oligo/polymeric products of MG catalyzed by carnosine or anserine. MG toxicity (0.3-1 mM) was dose-dependent for podocytes, tubular and mesangial cells whereas low MG levels (0.2 mM) resulted in increased cell viability in podocytes (143±13%, $p<0.001$) and tubular cells (129±3%, $p<0.001$). Incubation with carnosine/anserine did not reduce MG-induced toxicity, independent of incubation times and across large ranges of MG to carnosine/anserine ratios. Cellular carnosine uptake was low (<0.1% in 20 hours) and cellular carnosine concentrations remained unaffected. The putative carnosine transporter PHT1 along with the taurine transporter (TauT) was expressed in all

T. Weigand and B. Singler contributed equally to this paper.

Verena Peters
Center for Pediatrics and Adolescent Medicine, Im Neuenheimer Feld 669, Heidelberg (Germany)
Tel. +49-6221-5631715, E-Mail Verena.Peters@med.uni-heidelberg.de

cell types while PEPT1, PEPT2 and PHT2, also belonging to the proton-coupled oligopeptide transporter (POT) family, were only expressed in tubular cells. ***Conclusion:*** While carnosine and anserine catalyze the formation of MG oligo/polymers, the molar ratios required for protection from MG-induced cellular toxicity are not achievable in renal cells. The effect of carnosine *in vivo*, to mitigate diabetic nephropathy may therefore be independent upon its ability to scavenge MG and/or carnosine is mainly acting extracellularly.

Introduction

Diabetic nephropathy (DN) is the most common cause of end-stage renal disease in the Western world. Despite increasing knowledge on the pathogenesis of DN and potential therapeutic interventions, progression to end-stage renal disease still occurs in a substantial number of diabetic patients. Tight control of blood glucose continues to be the primary treatment option, but only partially prevents the manifestation of late complications and with large inter-individual variations [1, 2]. Substantial research has linked the highly reactive, glucose-derived metabolite methylglyoxal (MG) to diabetic complications [3, 4]. MG is a potent glycating agent [5] leading to the formation of advanced glycation end products (AGEs) [6] and is formed by the non-enzymatic dephosphorylation of triosephosphates [7, 8]. The formation of the MG-derived AGE and MG-derived hydroimidazolone isomer 1 (MG-H1) correlates with the development of diabetic complications such as DN [9]. Reactive metabolites such as MG are considered secondary messengers of free radicals that act both as signaling molecules and cytotoxic products of lipid peroxidation causing long-lasting biological consequences, in particular by covalent modification of macromolecules [10]. Reducing MG concentrations and antagonizing MG actions is a promising means to prevent diabetic complications [11]. The histidine-containing dipeptide carnosine is able to quench reactive carbonyl species such as MG or the α, β-unsaturated aldehyde 4-hydroxy-*trans*-2-nonenal (HNE) [12, 13]. Carnosine acts through two reactive moieties, one of the nitrogen atoms of the imidazole ring or the amino group nitrogen of the β-alanine residue. These nucleophilic nitrogens target the two reactive sites of α, β-unsaturated aldehydes, the aldehyde function or the electrophilic C3 atom [14]. Cellular uptake of carnosine occurs by proton-coupled oligopeptide transporters (POTs), membrane proteins that translocate various small peptides and peptide-like drugs across the biological membrane via an inwardly-directed proton gradient and negative membrane potential [15]. At present, four members of the POT family, namely PEPT1 (SLC15A1), PEPT2 (SLC15A2), PHT1 (SLC15A4) and PHT2 (SLC15A3), have been identified in mammals [16]. Unlike PEPT1 and PEPT2, PHT1 [17] and PHT2 also transport a single amino acid, L-histidine, in addition to the proton-stimulated transport of di- and tripeptides. The uptake of β-alanine, the precursor of carnosine, is largely driven by a Na^+/Cl^- dependent taurine transporter (TauT, SLC6A6) [18].

In diabetic mice, carnosine supplementation mitigates DN, reduces renal vasculopathy [2], normalizes vascular permeability [2] and improves wound healing [19]. In streptozotocin-induced diabetic rats, carnosine treatment prevents apoptosis of glomerular cells, podocyte loss [20, 21] and vascular damage [22]. In patients with type 2 DM we recently demonstrated an association of the susceptibility to develop DN with a polymorphism in the carnosinase 1 gene CNDP1 [23-25]. The kidney has an intrinsic carnosine metabolism with carnosine synthase and carnosinase 1 (CN1) being expressed in glomeruli and tubular cells [26]. CN1 activity is increased under diabetic conditions [27]. Carnosine uptake into renal cells occurs by the proton-coupled oligotransporter PEPT2 [16].

We now provide evidence that carnosine efficiently catalyzes the formation of MG oligo/polymeric products and prevents the formation of AGEs, but at molar ratios to cytotoxic MG concentrations which exceed amounts tolerated by renal cells and which are unable to be reached by cellular carnosine uptake in any case.

Materials and Methods

Chemicals were purchased from Sigma-Aldrich (Munich, Germany) unless indicated otherwise.

Quenching of MG by carnosine

Carnosine, anserine (obtained from Bachem AG, Switzerland) and MG were incubated in a 1:1 molar ratio in 100 mM sodium phosphate buffer at pH 7.4 with final concentrations of 10 mM. *tert*-Butyloxycarbonyl lysine (BocLys), lysine with a *tert*-butyloxycarbonyl protecting group, was used as a control due to being able to rapidly react with MG and form AGEs [28]. The reaction was followed by absorbance measurement at 336 nm for formation of the products for 8 hours with measuring intervals of 5 minutes.

NMR spectra

NMR spectra were acquired at 25°C using a Bruker Avance II NMR spectrometer equipped with a 5-mm inverse-configuration probe with triple-axis-gradient capability at a field strength of 14.1 T operating at 600.1 MHz for ^{1}H and 150.9 MHz for ^{13}C nuclei. Pulse widths were calibrated following the described protocol [29]. Chemical shifts (δs) are reported relative to the internal standard 3-(trimethylsilyl) propionic-2, 2,3, 3-d4 acid sodium salt (TSP) for which δ_H=0 ppm and δ_C=0 ppm. General NMR experimental and acquisition details including the 1D NOESY pulse sequence with pre-saturation for water suppression, selective saturation transfer (saturation time 5 seconds) and T_2 filter with pre-saturation (τ_{lock} 1.2 seconds) and standard gradient-selected 2D COSY, HSQC and HMBC spectra with pre-saturation have been previously described [30, 31]. For time-course experiments, samples were accurately weighed and made up volumetrically to 500 µl to provide 50 mM solutions of both MG and the amino acid/dipeptide using aqueous sodium phosphate buffer (375 µl, 100 mM, pH 7.4) and D_2O (125 µl) containing TSP while samples for signal assignment were prepared similarly but with nominal dispensation. Following preparation, solutions were transferred to 5-mm NMR tubes for immediate measurement.

NMR data

MG non-hydrated form (<0.05% relative to total MG). ^{1}H NMR: 9.452 (s, H1), H3 not found. MG monohydrate (61% relative to the dihydrate only). ^{1}H NMR: 5.284 (s, H1), 2.305 (s, 3H, H3). ^{13}C NMR: 211.99 (C2), 92.68 (C1), 27.37 (C3). MG dihydrate (39% relative to the monohydrate only). ^{1}H NMR: 4.816 (s, H1, δ_H taken from the HSQC spectrum due to overlap with the HDO signal), 1.377 (s, 3H, H3). ^{13}C NMR: 98.11 (C2), 94.89 (C1), 24.34 (C3). Oligo/polymeric species were not structurally identified but ^{1}H methyl signals at 1.472, 1.476, 1.482, 1.507, 1.518, 1.541, 1.544, 1.551 and 1.652 ppm were shown to belong to such species by 1D selective saturation transfer.

MG modification of proteins

Quantification of MG modification of proteins was performed according to Ahmed et al. [32]. In brief, human serum albumin was incubated with MG in a ratio of 1:10, respectively. Carnosine or anserine were added in ratios of 1:1; 2:1; 10:1; 20:1; 100:1; 200:1 and 1, 000:1 to MG. Incubation was performed at 37°C with continuous shaking for 24 hours. For purification, the modified proteins were concentrated by centrifugal filtration with a 10 kDa cut-off filter and washed three times with 50 mM ammonium carbonate buffer. The washed proteins were collected and transferred to a glass vial and lyophilized to dryness. Protein samples were analyzed either by SDS-PAGE and Western blot for *N*-carboxyethyl lysine (CEL) or by ELISA for MG-derived AGEs. For analysis by Western blot, 0.5 µg of protein were denatured in Laemmli buffer, resolved by SDS-PAGE (4 - 15% Mini-PROTEAN TGX, Biorad, Hercules, CA) and transferred onto a nitrocellulose membrane and blocked using 2% milk powder in PBS and 0.05% Tween 20 (PBS-T) at room temperature for 1hr. Membranes were then incubated overnight at 4°C with antibodies against CEL (1:500 dilution, CEL025, mouse, Biologo) and Albumin (1:10,000 dilution, 4929, rabbit, Cell Signaling Technology) in 2% milk powder in PBS-T. Blots were washed and then incubated with an appropriate HRP-conjugated antibody (1:2000 in 2% milk powder in PBS-T) for 1 hour at room temperature. Proteins were visualized on X-ray films using ECL detection reagents (GE Healthcare, Buckinghamshire, UK) with varying exposure times (0.1–2 min). The measurement of the content of the MG-derived AGEs was performed using a competitive ELISA, according to the manufacturer's instructions (OxiSelect Methylglyoxal Competitive ELISA, STA-811, Cell Biolabs, San Diego, CA).

For measurement of MG-H1 formation by Western blot, tubular cell samples were lysed in RIPA-buffer (radioimmunoprecipitaion assay buffer: 150 mM NaCl, 0.1 % Triton X-100, 0.5 % sodiumdeoxycholate, 0.1 % SDS, 50 mM Tris-HCl (pH 8.0) and one proteaseinhibtor cocktail tablet (cOmplete tablets, Mini EASYpack, Roche Diagnostics, Mannheim, Germany) per 15 ml) and separated by SDS-PAGE in 8% polyacrylamide gels (Twin-Plate Mini Gel Unit, Carl Roth GmbH + Co. KG, Karlsruhe, Germany). Samples were transferred to a nitrocellulose membrane by semi-dry blot. The membrane was blocked with protein-free blocking buffer (Pierce Protein-free Blocking Buffer, Thermo Fisher Scientific, Waltham, MA) for 1 hour at room temperature and incubated with anti-MG-H1 antibody (1:400 in protein-free blocking buffer) at 4°C over night and after washing incubated with a secondary HRP-conjugated antibody (1:1000 in protein-free blocking buffer). Western blots were developed with Clarity Western ECL Substrate (Biorad, Hercules, CA) and visualized by a fluourescence imaging system (PEQLAB fusion, PEQLAB, Erlangen, Germany).

Cell culture

Conditionally immortalized murine podocytes (ImmortoMouse, Charles River, Wilmington, MA) were grown in RPMI 1640 medium (Thermo Fisher Scientific, Waltham, MA) with 10% (v/v) fetal calf serum (Biochrom, Berlin, Germany) and 1% penicillin and streptomycin (v/v) (Thermo Fisher Scientific, Waltham, MA) with 10 U/µl γ-interferon (Roche Diagnostics, Mannheim, Germany) at 33°C with 5% CO_2 on collagen type I (BD Biosciences, Bedford, MA) coated flasks. Cells were then detached with trypsin (Thermo Fisher Scientific, Waltham, MA) and seeded at 5, 000 cells per cm^2 to allow them to differentiate for 12-14 days at 37°C with 5% CO_2 in growth medium without γ-interferon. Immortalized human tubular cells (HK-2; American Type Culture Collection CRL-2190) and immortalized murine mesangial cells (Mes13; American Type Culture Collection CLR-1927) were grown in RPMI 1640 medium with 10 % fetal calf serum (v/v) and 1% penicillin and streptomycin (v/v) at 37°C with 5% CO_2.

Cell viability

Cell viability was measured with MTT assay. In brief, confluent cells were detached with trypsin (Thermo Fisher Scientific, Waltham, MA) and seeded on 96-well plates followed by an additional growth phase for 24 hours. For short-term experiments cells were then treated with MG and carnosine for a further 48 hours, or 7 days (tubular cells) or 14 days (podocytes) for long-term incubations. Media were changed every three days. At the end of the incubation period, 50 µl PBS (Thermo Fisher Scientific, Waltham, MA) with 2 mg/ml 3-(4, 5-dimethylthiazol-2-yl)-2, 5-diphenyltetrazolium bromide (MTT) was added to each well. This compound is converted to purple formazan crystals by metabolically active cells. After 4 hours, the medium was discarded and cells were lysed with 200 µl DMSO per well for 1 hour. The absorption of the solution was measured spectrophotometrically at 590 nm, the absorption maximum of formazan crystals.

Carnosinase activity and carnosine and anserine levels

Cells were harvested by adding 60 µl pre-lysis buffer containing 20 mM Tris/HCl (pH 8.9, 150 mM NaCl, 20 mM NaF and 1% Triton) for detection of CN1 activity and additionally 2 mM EDTA was added for measurement of anserine and carnosine levels.

CN1 activity was assayed as described previously [33]. In brief, the reaction was initiated by the addition of 1 mM carnosine to cell homogenate at pH 7. The reaction was terminated at pre-determined intervals (every 5 minutes) by adding 1% trichloroacetic acid. Liberated histidine was derivatized by adding *o*-phthalaldehyde and the fluorescence measured using a MicroTek plate reader (λ_{Ex}:360 nm; λ_{Em}: 460 nm).

Anserine and carnosine concentrations were measured fluorometrically using HPLC as previously described [34]. The homogenized cells were diluted with sulfosalicylic acid and derivatized using carbozole-9-carbonyl chloride, applied to a Jupiter column (C18, 300 Å, 5 µm particle size, 250 x 4.6mm) and detected by fluorescence detection (Shimadzu RF-20A) at λex 287 nm/λem 340 nm. The mobile phase consisted of solution (A) 50 mM acetate buffer in distilled water, pH 4.37 and solution (B) a mixture of acetonitrile, methanol and tetrahydrofuran 70:25:5 (v/v/v). The solutions were degassed prior to use. All samples were measured at least twice and one sample was spiked with standards to definitively identify each analyte. The reliability of the method was 0.91.

SOD activity

Superoxide dismutase activity of all three types of SOD (Cu/Zn, Mn and FeSOD) was measured with renal cell lysate using Superoxide Dismutase Assay Kit (Cayman Chemical Company, Ann Arbor, MI) according to the manufacturer's manual.

Table 1. PCR Primer used for qPCR.

Primer		Sequences		
GPX1	-fw	TTCATGCTCTTCGAGAAGTGCGAGG	-rev	ACATCGTTGCGACACA
SOD2	-fw	CAGATAGCTCTTCAGCCTGC	-rev	CAGTGGATCCTGATTT
RPI32	-fw	AGGCATTGACAACAGGGTTC	-rev	GTTGCACATCAGCAGC
SLC15A1	-fw	ATGTGGCTTCAATTTCACCT	-rev	GTTAAGACCATCCTTT
SLC15A2	-fw	CTTCTGGTTCTTATCTTCATCCC	-rev	ATACTGTTCCCATCTT
SLC15A3	-fw	CTTCACCTCCACATCCCAAA	-rev	GCTGGCAAAGATCTCA
SLC15A4	-fw	GAGTCTTCATTTGAGGATTCCA	-rev	AGCTGAGTATGCAAAT
SLC15A5	-fw	GGATGGATTTCTTCTGCCGA	-rev	GAGATGAGATATACCA

GSH concentration

The concentration of reduced glutathione (GSH) was determined in renal cells using a Quantichrome Glutathione Assay kit (Bioassay Systems, Hayward, CA) following the manufacturer's instructions.

Expression of glutathione peroxidase, SOD and carnosine transporter

RNA purification was performed with RNeasy Minikit (Quiagen, Venlo, Netherlands) with samples being treated with DNase I (Roche, Basel, Switzerland) for degradation of genomic DNA. Purified RNA was transcribed to cDNA via EpiScript reverse transcriptase (Biozym, Oldendorf, Germany) and non-specific random hexamere primers (Thermo Fisher Scientific, Waltham, MA). Expression of the genes of interest (GPx-1, SOD2 and putative carnosine transporters PEPT1, PEPT2, PHT1 and PHT2) was then analyzed with specific primer pairs via quantitative real time polymerase chain reaction (qPCR) as described before [35]. Table 1 shows the utilized PCR primers.

Carnosine uptake

For the carnosine uptake measurement, renal cells were seeded at densities of 10, 000 cells per well for tubular and mesangial cells and 25, 000 cells per well for podocytes on a 96-well plate in 200 µl of growth medium. Cells were allowed to adhere overnight at 37°C after which medium was removed and the cells washed with PBS. Krebs-Ringer-HEPES (KRH) buffer was added (180 µl per well) and 20 µl of [^{3}H]-L-carnosine (Hartmann Analytic, Braunschweig, Germany), solved in KRH buffer, for 0, 5, 10, 25, 50 and 100 µM final concentrations. The cells were further incubated at 37°C for 20 hours, then washed twice with ice-cold PBS. Either KRH buffer (20 µl per well with cells) or carnosine solution (20 µl per well without cells) was added. After the addition of 200 µl of MicroScint-O scintillation liquid (PerkinElmer, Waltham, MA) to each well and 60 minutes of incubation, the ^{3}H signal was measured with a TopCount NXT microplate scintillation and luminescence counter (Packard, Meriden, CT).

Statistical analysis

Data were obtained from at least 3 independent experiments while cell viability data were obtained from at least 3 independent experiments comprising at least 5 measurements per data point. Data are given as mean and standard deviation (SD). Effects of MG, carnosine and anserine on cell viability were analyzed with a multiple regression approach. Post-hoc comparisons were computed using least-square means with Dunnett's contrasts (e.g. the control group were compared to each of the other experimental condition) implemented in Lenth [36]. Effect graphics based on effects-package for R [37]. All statistical analysis were computed with R. A p-value of ≤0.05 was considered significant.

Results

Scavenging potential of MG and prevention of AGE formation in cell free system

To first evaluate the quenching activity of MG, the absorbance at 336 nm in a cell free environment was measured after co-incubation of MG with carnosine and anserine for 8 hours (ratio 1:1, 10 mM final concentration). The absorbance at 336 nm increased in a time-dependent manner and was higher for carnosine than for anserine, the latter being comparable with the effect seen for BocLys which served as a quenching control (Fig. 1A). The color of

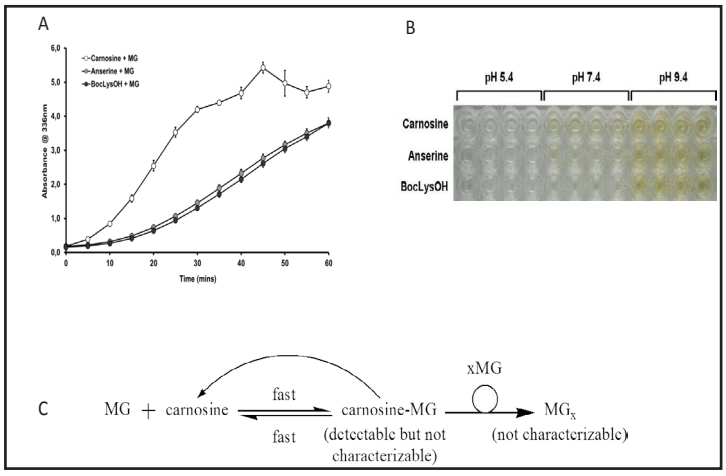

Fig. 1. MG quenching in a cell-free environment by UV-vis. Carnosine, anserine and BocLys were co-incubated with MG (1:1 ratio). The absorbance at 336 nm increased in a time-dependent manner (A) indicating quenching of MG. The change in the solutions from clear to a yellow-brownish color was pH dependent (B). The possible reaction sequence of MG in the presence of carnosine as discerned by ^{1}H NMR analysis: MG and carnosine react to form transient adducts. MG reacts further to form oligo/polymeric products while carnosine is released and remains on the whole unaltered. The same reaction sequence can be construed for anserine, BocLys and imidazole in place of carnosine. (C).

the solutions changed from clear to brownish yellow (Fig. 1B) in each case and the reaction was enhanced by increasing pH. The color change is indicative of the Maillard reaction and the consumption of free MG. The effects were more prominent for carnosine as compared to both BocLys and anserine. To investigate the reactions further, ^{1}H NMR analysis was conducted.

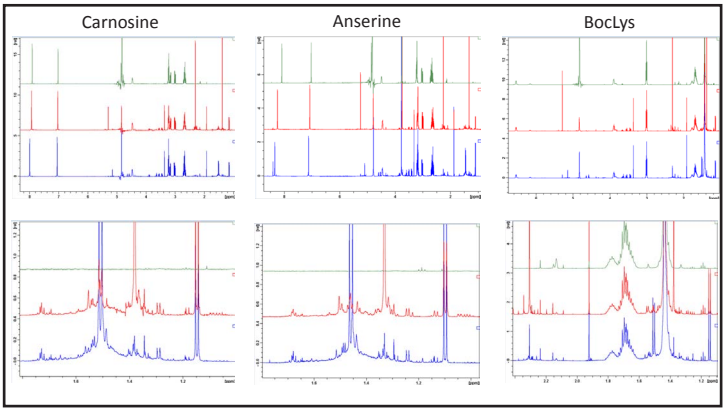

Fig. 2. Time-course ^{1}H NMR analysis of the treatment of MG with carnosine, anserine and BocLys. ^{1}H NMR analysis identified the mono- and dihydrates of MG and various oligo/polymeric MG species by selective saturation of the ^{1}H methyl signals and acquisition with a T_2 filter. The growth of oligo/polymeric MG products concomitant with the consumption of free MG is clearly evident in the expanded upfield portions of the spectra in each case (lower row of panels) while signals attributed to transient MG-adducts were also observed (not shown in expanded detail but evident for carnosine and anserine in the downfield region of the spectra) and identified by selective saturation experiments. In each case, the top trace (green) within each panel is the ^{1}H NMR spectrum of just the amino acid/dipeptide, the middle trace (red) is the first spectrum of the incubation with MG and the bottom trace (blue) is the final spectrum of the incubation with MG.

By ^{1}H NMR analysis of the co-incubation of MG with either carnosine or anserine, only transient MG-carnosine and MG-anserine adducts (Fig. 1C) were detected and only in very low concentrations prior to the gradual and significant accumulation of oligo/polymeric products of MG evident in the ^{1}H NMR spectra (Fig. 2) concomitant with the consumption of free MG while the majority of carnosine/anserine on the whole remains unaltered. These observations are consistent with the aforementioned color changes. Since the MG adducts were present in only very low concentrations and are transient species which could not be isolated and they only provided broad signals in the NMR, they could not be fully characterized and their structures determined. Their formation was clear though, by both the appearance of new signals,

albeit at low intensities, and by their catalytic effect on the formation of oligo/polymeric products of MG as well as the observation of saturation transfer from the aromatic signals of the dipeptides. Whether these transient adducts are directly involved in the catalysis as depicted in Fig. 2 is only a presumption but notwithstanding that stable 1:1 adducts between MG and carnosine or anserine were not formed. The signals attributed to oligo/polymeric products of MG were shown to be high-molecular weight species by the application of a T_2 filter and were similarly shown to be in a dynamic equilibrium with the various free MG species (the non-hydrated form, the monohydrate and the dihydrate) by saturation transfer experiments from the ^1H methyl signals of free MG. Co-incubations of MG with BocLys (Fig. 2) and imidazole were also examined for comparison and provided similar results to the co-incubation of MG with carnosine or anserine. Thus, the reaction with BocLys shows that the amine group nitrogen reacts with MG, while reaction with imidazole shows that one of the imidazole nitrogens reacts with MG. Hence carnosine can potentially react with MG either via the amine group nitrogen or one of the imidazole nitrogens. For N-methylated carnosine, i.e. anserine, both imidazole nitrogens are blocked, i.e. non-reactive, and therefore reaction is slower. Thus, the free imidazole nitrogen reacts faster than the amine group nitrogen and hence the reaction order carnosine > anserine > BocLys is rationalized. Times for half of the MG to be consumed in the reactions were 0.6, 2.4 and 5.8 hours for carnosine, anserine and BocLys, respectively (data not shown).

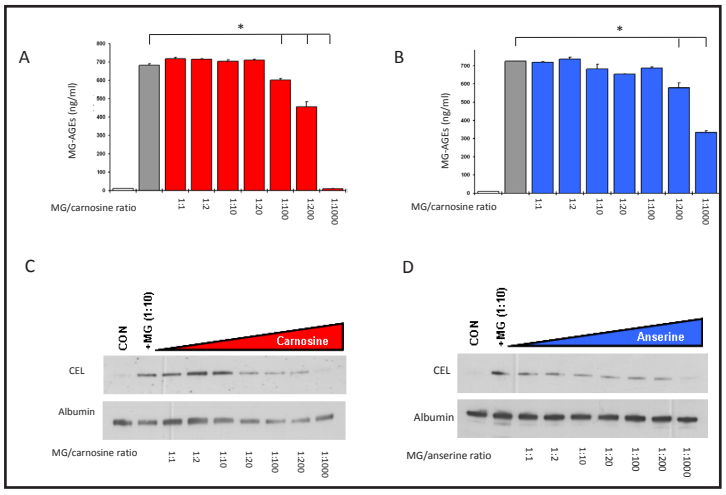

Fig. 3. Carnosine and anserine prevent MG-induced AGE and CEL formation. Human serum albumin was treated with MG (1:10 ratio) for 24 hours. Carnosine and anserine were added with increasing concentrations. Carnosine was able to prevent AGE formation (A) significantly at a ratio of 100:1 to MG while anserine (B) required a ratio of 200:1 to MG ($p<0.05$). Carnosine was able to prevent N-carboxyethyl lysine formation significantly at a ratio of 20:1 (C) to MG while anserine (D) only required a ratio of 1:1 to MG for significant inhibition to occur.

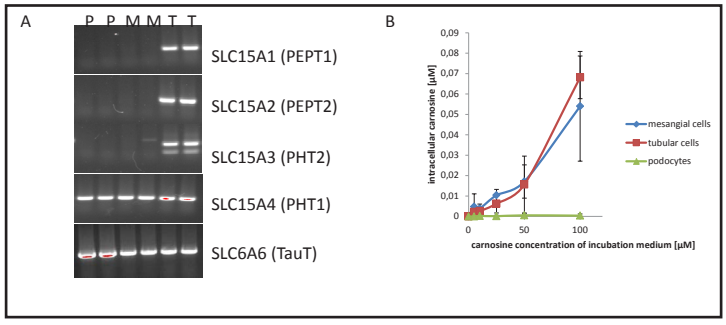

Fig. 4. Carnosine uptake in renal cells. The putative transporters of carnosine (A), PEPT2, PEPT1 and PHT2, were only expressed in tubular cells while PHT1 and Taut were all expressed in mesangial cells (M), podocytes (P) and tubular cells (T). The uptake of radiolabeled carnosine for tubular cells and mesangial cells was very low and no uptake was detectable for podocytes. The average uptake was 0.04±0.02% for tubular cells and 0.05±0.02% for mesangial cells (B).

The formation of AGEs derived from human serum albumin in the presence of MG was significantly inhibited by the addition of carnosine at a ratio of 100:1 to MG (Fig. 3A); for anserine, a higher ratio to MG of 200:1 was required for significant inhibition (Fig. 3B). To reduce AGE formation by 50%, a carnosine to MG ratio of 400:1 and an anserine to MG ratio

of 700:1 were required. *N*-carboxyethyl lysine (CEL) formation from human serum albumin and MG was also reduced dose-dependently by carnosine or anserine. Their reduction of CEL was even more effective with MG to carnosine (Fig. 3C) and MG to anserine (Fig. 3D) ratios of as little as 1:20 and 1:1, respectively, decreasing CEL formation significantly.

Table 2. EC_{50} values (n=3) for tubular cells, podocytes and mesangial cells after incubation with carnosine, anserine and MG for 48 hours

	EC_{50} (mM)		
	Tubular Cells	Podocytes	Mesangial Cells
Carnosine	4.1	9.1	3.7
Anserine	3.2	4.7	6.0
MG	0.7	1.4	0.1

Cellular carnosine transporter expression and carnosine uptake

Quantitative PCR demonstrated that PHT1, one of four known proton-dependent oligopeptide transporters (POTs), together with taurine transporter (TauT) which transports β-alanine, was expressed in tubular, mesangial cells and podocytes. The three other POTs, i.e. PEPT1, PEPT2 and PHT2, were only expressed in tubular cells (Fig. 4A). Uptake of radiolabeled carnosine after 20 hours of incubation was only minor in tubular cells and mesangial cells and almost absent in podocytes (Fig. 4B). Accordingly, intracellular carnosine concentrations hardly increased. Incubation with 0.1 mM radioactive carnosine for 20 hours increased intracellular carnosine concentrations for tubular cells only to 0.07±0.01 µM (p≤0.001) and for mesangial cells only to 0.05±0.03 µM (p≤0.05).

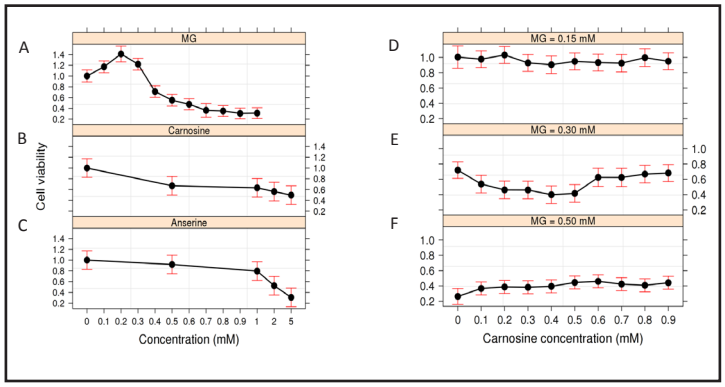

Fig. 5. Effects of carnosine, anserine and MG on cultured renal cells. Effects of carnosine (A), anserine (B) and MG (C) on the cell viability of tubular cells. Cell viability after 48 hours was determined by MTT assay. Tubular cells were then incubated with 0.15 mM (D), 0.3 mM (E) or 0.5 mM (F) methylglyoxal and increasing concentrations of carnosine for 48 hours. Cell metabolic activity was determined by MTT assay and compared to MG treated controls.

Effect of carnosine and anserine on MG-induced cell toxicity

Podocytes, tubular and mesangial cells tolerate carnosine and anserine in high concentrations but to different degrees (Table 2). Carnosine was tolerated best by podocytes whereas the tolerances by tubular (Fig. 5A) and mesangial cells of carnosine were less. Mesangial cells tolerated anserine at higher concentrations as compared to podocytes and tubular cells (Fig. 5B). Exposure to 0.15 mM MG had no effect on cell viability whereas levels above 0.2 mM resulted in a dose-dependent decrease of cell viability (Fig. 5C) for all three renal cell types in comparison to controls. MG was tolerated by podocytes at higher concentrations in comparison to tubular and mesangial cells. Exposure to 0.2 mM MG increased cell viability for tubular cells by 29%±3.4% (p<0.001) and for podocytes by 43%±12.7% (p<0.001), but not for mesangial cells.

Renal cells were then exposed to MG (0.15, 0.3 and 0.5 mM) with increasing concentrations of carnosine and anserine (0.1-0.9 mM). Exposure of tubular cells to 0.15 mM MG (Fig. 5D) had no effect on cell viability independently of the amount of carnosine or anserine added. Exposure to 0.3 mM MG (Fig. 5E) decreased cell viability significantly for carnosine concentrations ranging from 0.2 to 0.5 mM (p<0.01, Dunnet contrasts) while higher carnosine

levels had no effect on cell viability. The addition of 0.5 mM MG (Fig. 5F) reduced cell viability to 26.2±16.1% ($p<0.05$, Dunnet contrasts). The addition of 0.5 and 0.6 mM carnosine increased cell viability at a 6% significance level. In podocytes, no beneficial effect of carnosine (0.1 - 0.9 mM) on MG-induced stress (0.15, 0.3 and 0.5 mM) was detected via Dunnet contrasts. Co-incubation of podocytes with 0.5 mM anserine and 0.15 mM MG even reduced cell viability to 79.6±6.5% compared to the untreated control ($p=0.01$, Dunnet contrasts). Likewise, extension of MG and carnosine co-incubation to 7 days (tubular cells) and 14 days (podocytes) did not consistently reduce MG-induced cell toxicity. Co-incubation with the carnosine precursor histidine and β-alanine (1:1 ratio, 0-1.0 mM) with 0.4 mM MG for 48 hours also had no protective effect on MG-induced cell toxicity in mesangial cells, higher levels of β-alanine and histine (1.5 mM/ even decreased cell by proliferation about 7% (66.6±8.9%, $p< 0.05$).

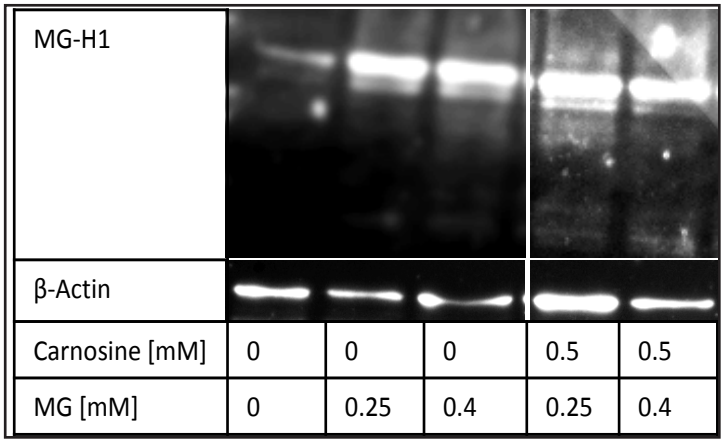

Fig. 6. Formation of MG-H1. Tubular cells were incubated with 0.25 mM or 0.4 mM MG for 6 hours. The formation of MG-H1 through carbonylation of arginine residues by MG was not altered by the addition of 0.5 mM carnosine.

Effect of MG on CN1 activity

The incubation of tubular cells with MG increased intracellular CN1 activity. Incubation with 0.5 mM MG increased CN1 activity from 2.1±0.2 to 3.5±0.3 µmol/mg/h ($p<0.05$). Intracellular carnosine and anserine varied greatly with a mean of 3.6 nmol/mg anserine and a standard deviation of 3.1 [95% CI 1.6-7.5] and a mean of 1.5 nmol/mg carnosine [95% CI 0.9-2.9]. MG-induced increased CN1 activity did not result in a significant decline in intracellular carnosine or anserine levels.

Effect of MG on oxidative stress parameter

In tubular cells, addition of 0.3 mM and 0.5 mM MG almost halved SOD2-expression, also known as manganese-dependent superoxide dismutase (MnSOD), within 24 hours to 62.3±24.1% ($p\leq0.05$) and 58.8±18.5% ($p\leq0.01$), respectively, compared to untreated controls and was not influenced by the addition of 0.5 mM carnosine. However, activity (7.69±1.44 U/mg) of all three types of SOD (Cu/Zn, Mn and FeSOD) was not influenced by incubation with 0.5 mM MG (7.16±1.28 U/mg) or 0.5 mM carnosine (7.16±0.87 U/mg; both p=ns). SOD activity in podocytes (15.75±2.09 U/mg) was neither significantly altered by incubation with 0.15, 0.3 or 0.5 mM MG (14.7±1.75 U/mg, 10.55±4.15 U/mg and 13.41±1.08 U/mg, respectively; all p=ns) nor by co-incubation with 0.5 mM MG and 0.5 mM carnosine (16.2±2.93 U/mg; p=ns).

Tubular cell glutathione peroxidase gene (GPx-1) expression was unchanged after 24 hours of incubation with 0.3 mM MG (95.8±40.3%), 0.5 mM carnosine (87.6±19.7%) or the combination of both (95.3±17.1% and 98.2±21.8%; all p=ns). GSH concentrations in tubular cells and podocytes remained in the same range with increasing levels of MG or carnosine or the combination of both (data not shown). Also, MG-H1 formation was not reduced by the addition of carnosine (Fig. 6).

Discussion

Reactive metabolites essentially contribute to the development of DN and the formation of the MG-derived MG-H1 closely correlates with the degree of DN [11, 38]. Recent studies have demonstrated the beneficial effects of carnosine on the development of diabetic complications [2, 19, 22, 27] and it is assumed that those effects are, at least partially, due to the MG-scavenging potential of carnosine. The quenching capacity and structure related reactivity of carnosine for reactive species has already been reported [39-41]. We therefore investigated the scavenging potential of carnosine and anserine on MG-toxicity in renal cells.

In summary, carnosine and anserine both prevented MG-induced AGE and CEL formation *in vitro* and NMR studies revealed that the two compounds catalyzed the formation of MG oligo/polymeric products, presumably via transient adducts between MG and carnosine/anserine that were observable in only very minor concentrations, rather than forming stable 1:1 MG adducts. These findings are in line with recent studies demonstrating poor quenching activity of carnosine derivatives towards MG [14, 42]. Quenching capacity of carnosine is higher against other reactive metabolites such as acrolein and HNE [14, 40, 41, 43]. Although both, HNE and MG, belong to the group of reactive carbonyl species reacting with the nucleophilic groups in proteins, the two compounds are chemically distinct with both very different reaction kinetics leading to different stable end products. Dicarbonyl derivatives such as MG are more likely involved in AGE formation, while α, ß-unsaturated carbonyls such as HNE generate advanced lipidoxidation end products (ALEs) [41]. Thus, the scavenging ability of carnosine or anserine against HNE, acrolein or other reactive compounds might be of higher relevance.

A protective effect on cell viability or oxidative stress markers of carnosine or anserine addition to MG-stressed renal cell cultures could not be observed, independent of the cell type, incubation times and MG to carnosine/anserine ratios. The different findings *in vitro* and *in vivo* might be caused by not achieving the required intracellular carnosine or anserine to MG ratios and/or carnosine is mainly acting extracellularly. In our experiments, *in vitro* CEL formation was reduced by MG to carnosine ratios of 1:20 and by MG to anserine ratios of 1:1. However, carnosine uptake was low in mesangial and tubular cells, almost absent in podocytes and remained below 1 μM for all cells within 20 hours and is probably not crucial for the beneficial effects reported earlier. Although the putative carnosine transporter PHT1 was expressed in all cell types, podocytes showed no carnosine uptake and the cell-specific role of all transporters needs further investigation. On the other hand, the dynamics of MG are faster. The majority of MG is either quickly bound to protein or was detoxified via the glyoxalase pathway involving glyoxylase I and II, metabolizing MG into lactate by using NADPH and GSH [44]. Previous findings showed peak formation of MG-H1 in endothelial cells already after 6 hours and that carnosine fails to prevent the formation of MG-H1 from human serum albumin *in vitro* [42]. In our experiments, the addition of carnosine did not reduce MG-H1 formation in renal cells.

Since intracellular carnosine levels varied but were hardly influenced by the quantity of carnosine added, carnosine and anserine may act extracellularly. Also the addition of the carnosine precursors β-alanine and histidine to the cells did not increase intracellular carnosine or anserine levels. The putative β-alanine transporter TauT is expressed in all renal cells and we previously demonstrated carnosine synthase (CS) expression in podocytes and tubular cells [26]. On the other hand, increased CN1 activity due to MG-induced carbonylation of the enzyme, as described before [27], also did not alter intracellular carnosine levels. Although we only found low carnosine transport into cells, all three cell types only tolerated a certain amount of carnosine or anserine. Whether the comparatively high tolerance of podocytes against carnosine is due to hardly any carnosine uptake into cells remains speculative. We used both human and mice kidney cells and cannot exclude that our cell lines may have lost parts of their original expression profiles. Reassuringly, CN1 and CS are both expressed in the kidney of human and mouse [26].

Although carnosine showed no protective effect against MG-induced toxicity, low MG levels (0.2 mM) resulted in increased cell viability in podocytes and tubular cells. A protective response in yeast and in mouse cardiac endothelial cells via the initiation of cellular defense mechanism was recently reported [45, 46]. The effectors of MG defense include heat shock proteins and proteins involved in mitochondria-associated protein degradation. No protective effect of MG was detectable for mesangial cells which are particularly sensitive to MG. MG and MG end products CEL and MG-H1 have been reported [9] to be involved in the progression of DN, thus the different sensitivity of renal cell types towards MG might be considered to be a reflection of the pathomechanisms of early DN *in vivo*. Besides podocyte loss, which seems to be an important pathological feature in DN, hypertrophy of mesangial cells [47] seems to be of importance in the progression of DN and might be caused by MG-induced toxicity.

Conclusion

Taken together, *ex vivo* carnosine prevents MG-induced CEL formation but *in vivo* the mechanism of action is unlikely to be through intracellular MG scavenging. Cellular uptake and intracellular synthesis of carnosine and anserine are too low to achieve the concentrations required for efficient quenching and/or MG polymer formation in order to prevent MG-dependent MG-H1 and AGE generation and to preserve renal cell viability. Other mechanisms must be active to explain the repeatedly observed nephroprotective action of carnosine supplementation in diabetic rodents and the observed association of CN1 activity defining CNDP1 genotypes and the risk of nephropathy in diabetic humans. The function of carnosine as an antioxidant, as discussed in the literature [48-52], is controversial and its role in diabetes requires further investigation.

Abbreviations

AGE (Advanced glycation end product); CEL (*N*-carboxyethyl lysine); CN1 (Carnosinase 1); CNDP1 (Carnosinase 1 gene); DN (Diabetic nephropathy); HNE (4-hydroxy-trans-2-nonenal); MG (Methylglyoxal); MG-H1 (MG-derived hydroimidazolone isomer 1); POT (proton-coupled oligopeptide transporter); TauT (Taurine transporter).

Acknowledgements

This work was supported by the Deutsche Forschungsgemeinschaft (DFG, SFB 1118).

All authors were involved in planning this article, interpretation of literature, and in drafting and critically revising the manuscript. All authors reviewed the final manuscript and gave approval for submission. We thank Kristina Klingbeil for excellent technical assistence.

Disclosure Statement

The authors declare that they have no conflict of interest.

References

1 Fleming T, Nawroth PP: Reactive metabolites as a cause of late diabetic complications. Biochem Soc Trans 2014;42:439-442.

2 Peters V, Schmitt CP, Zschocke J, Gross ML, Brismar K, Forsberg E: Carnosine treatment largely prevents alterations of renal carnosine metabolism in diabetic mice. Amino Acids 2012;42:2411-2416.

3 Schalkwijk CG: Vascular AGE-ing by methylglyoxal: the past, the present and the future. Diabetologia 2015;58:1715-1719.
4 Jensen TM, Vistisen D, Fleming T, Nawroth PP, Rossing P, Jorgensen ME, Lauritzen T, Sandbaek A, Witte DR: Methylglyoxal is associated with changes in kidney function among individuals with screen-detected Type 2 diabetes mellitus. Diabet Med 2016;33:1625-1631.
5 Richard JP: Mechanism for the formation of methylglyoxal from triosephosphates. Biochem Soc Trans 1993;21:549-553.
6 Beisswenger PJ: Methylglyoxal in diabetes: link to treatment, glycaemic control and biomarkers of complications. Biochem Soc Trans 2014;42:450-456.
7 Fleming T, Cuny J, Nawroth G, Djuric Z, Humpert PM, Zeier M, Bierhaus A, Nawroth PP: Is diabetes an acquired disorder of reactive glucose metabolites and their intermediates? Diabetologia 2012;55:1151-1155.
8 Rabbani N, Thornalley PJ: Dicarbonyl stress in cell and tissue dysfunction contributing to ageing and disease. Biochem Biophys Res Commun 2015;458:221-226.
9 Beisswenger PJ, Howell SK, Russell GB, Miller ME, Rich SS, Mauer M: Early Progression of Diabetic Nephropathy Correlates With Methylglyoxal-Derived Advanced Glycation End Products. Diabetes Care 2013;36:3234-3239.
10 Jaganjac M, Tirosh O, Cohen G, Sasson S, Zarkovic N: Reactive aldehydes--second messengers of free radicals in diabetes mellitus. Free Radic Res 2013;47:S39-48.
11 Beisswenger PJ, Drummond KS, Nelson RG, Howell SK, Szwergold BS, Mauer M: Susceptibility to diabetic nephropathy is related to dicarbonyl and oxidative stress. Diabetes 2005;54:3274-3281.
12 Boldyrev A, Severin SE: The histidine-containing dipeptides, carnosine and anserine: distribution, properties and biological significance. Adv Enzyme Regul 1990;30:175-194.
13 Boldyrev AA, Aldini G, Derave W: Physiology and pathophysiology of carnosine. Physiol Rev 2013;93:1803-1845.
14 Colzani M, De Maddis D, Casali G, Carini M, Vistoli G, Aldini G: Reactivity, Selectivity, and Reaction Mechanisms of Aminoguanidine, Hydralazine, Pyridoxamine, and Carnosine as Sequestering Agents of Reactive Carbonyl Species: A Comparative Study. ChemMedChem 2016;11:1778-1789.
15 Daniel H, Kottra G: The proton oligopeptide cotransporter family SLC15 in physiology and pharmacology. Pflugers Arch 2004;447:610-618.
16 Jappar D, Hu Y, Keep RF, Smith DE: Transport mechanisms of carnosine in SKPT cells: contribution of apical and basolateral membrane transporters. Pharm Res 2009;26:172-181.
17 Yamashita T, Shimada S, Guo W, Sato K, Kohmura E, Hayakawa T, Takagi T, Tohyama M: Cloning and functional expression of a brain peptide/histidine transporter. J Biol Chem 1997;272:10205-10211.
18 Rasmussen RN, Lagunas C, Plum J, Holm R, Nielsen CU: Interaction of GABA-mimetics with the taurine transporter (TauT, Slc6a6) in hyperosmotic treated Caco-2, LLC-PK1 and rat renal SKPT cells. Eur J Pharm Sci 2016;82:138-146.
19 Ansurudeen I, Sunkari VG, Grunler J, Peters V, Schmitt CP, Catrina SB, Brismar K, Forsberg EA: Carnosine enhances diabetic wound healing in the db/db mouse model of type 2 diabetes. Amino Acids 2012;43:127-134.
20 Peters V, Riedl E, Braunagel M, Hoger S, Hauske S, Pfister F, Zschocke J, Lanthaler B, Benck U, Hammes HP, Kramer BK, Schmitt CP, Yard BA, Koppel H: Carnosine treatment in combination with ACE inhibition in diabetic rats. Regul Pept 2014;194-195:36-40.
21 Riedl E, Pfister F, Braunagel M, Brinkkotter P, Sternik P, Deinzer M, Bakker SJ, Henning RH, van den Born J, Kramer BK, Navis G, Hammes HP, Yard B, Koeppel H: Carnosine prevents apoptosis of glomerular cells and podocyte loss in STZ diabetic rats. Cell Physiol Biochem 2011;28:279-288.
22 Pfister F, Riedl E, Wang Q, vom Hagen F, Deinzer M, Harmsen MC, Molema G, Yard B, Feng Y, Hammes HP: Oral carnosine supplementation prevents vascular damage in experimental diabetic retinopathy. Cell Physiol Biochem 2011;28:125-136.
23 Janssen B, Hohenadel D, Brinkkoetter P, Peters V, Rind N, Fischer C, Rychlik I, Cerna M, Romzova M, de Heer E, Baelde H, Bakker SJ, Zirie M, Rondeau E, Mathieson P, Saleem MA, Meyer J, Koppel H, Sauerhoefer S, Bartram CR, Nawroth P, Hammes HP, Yard BA, Zschocke J, van der Woude FJ: Carnosine as a protective factor in diabetic nephropathy: association with a leucine repeat of the carnosinase gene CNDP1. Diabetes 2005;54:2320-2327.

24 Mooyaart AL, Zutinic A, Bakker SJ, Grootendorst DC, Kleefstra N, van Valkengoed IG, Bohringer S, Bilo HJ, Dekker FW, Bruijn JA, Navis G, Janssen B, Baelde HJ, De Heer E: Association between CNDP1 genotype and diabetic nephropathy is sex specific. Diabetes 2010;59:1555-1559.
25 Peters V, Zschocke J, Schmitt CP: Carnosinase, diabetes mellitus and the potential relevance of carnosinase deficiency. J Inherit Metab Dis 2018;41:39-48.
26 Peters V, Klessens CQ, Baelde HJ, Singler B, Veraar KA, Zutinic A, Drozak J, Zschocke J, Schmitt CP, de Heer E: Intrinsic carnosine metabolism in the human kidney. Amino Acids 2015;47:2541-2550.
27 Peters V, Lanthaler B, Amberger A, Fleming T, Forsberg E, Hecker M, Wagner AH, Yue WW, Hoffmann GF, Nawroth P, Zschocke J, Schmitt CP: Carnosine metabolism in diabetes is altered by reactive metabolites. Amino Acids 2015;47:2367-2376.
28 Degenhardt TP, Thorpe SR, Baynes JW: Chemical modification of proteins by methylglyoxal. Cell Mol Biol 1998;44:1139-1145.
29 Klika KD: The Application of Simple and Easy to Implement Decoupling Pulse Scheme Combinations to Effect Decoupling of Large Values with Reduced Artifacts. International Journal of Spectroscopy 2014;2014
30 Mäki J, Tähtinen P, Kronberg L, Klika KD: Restricted rotation/tautomeric equilibrium and determination of the site and extent of protonation in bi-imidazole nucleosides by multinuclear NMR and GIAO-DFT calculations. J Phys Org Chem 2005;18:240-249.
31 Virta P, Koch A, Roslund MU, Mattjus P, Kleinpeter E, Kronberg L, Sjöholm R, Klika KD: Synthesis, characterisation and theoretical calculations of 2, 6-diaminopurine etheno derivatives. Org Biom Chem 2005;3:2924-2929.
32 Ahmed N, Babaei-Jadidi R, Howell SK, Thornalley PJ, Beisswenger PJ: Glycated and oxidized protein degradation products are indicators of fasting and postprandial hyperglycemia in diabetes. Diabetes Care 2005;28:2465-2471.
33 Peters V, Kebbewar M, Jansen EW, Jakobs C, Riedl E, Koeppel H, Frey D, Adelmann K, Klingbeil K, Mack M, Hoffmann GF, Janssen B, Zschocke J, Yard BA: Relevance of allosteric conformations and homocarnosine concentration on carnosinase activity. Amino Acids 2010;38:1607-1615.
34 Schonherr J: Analysis of products of animal origin in feeds by determination of carnosine and related dipeptides by high-performance liquid chromatography. J Agric Food Chem 2002;50:1945-1950.
35 Cattaruzza M, Guzik TJ, Slodowski W, Pelvan A, Becker J, Halle M, Buchwald AB, Channon KM, Hecker M: Shear stress insensitivity of endothelial nitric oxide synthase expression as a genetic risk factor for coronary heart disease. Circ Res 2004;95:841-847.
36 Lenth RV: Least-squares means: the R package lsmeans. J Stat Softw 2016;69:1-33.
37 Fox J: Effect displays in R for generalised linear models. Journal of statistical software 2003;8:1-27.
38 Beisswenger PJ, Howell SK, Russell GB, Miller ME, Rich SS, Mauer M: Early progression of diabetic nephropathy correlates with methylglyoxal-derived advanced glycation end products. Diabetes Care 2013;36:3234-3239.
39 Aldini G, Orioli M, Rossoni G, Savi F, Braidotti P, Vistoli G, Yeum KJ, Negrisoli G, Carini M: The carbonyl scavenger carnosine ameliorates dyslipidaemia and renal function in Zucker obese rats. J Cell Mol Med 2011;15:1339-1354.
40 Vistoli G, De Maddis D, Straniero V, Pedretti A, Pallavicini M, Valoti E, Carini M, Testa B, Aldini G: Exploring the space of histidine containing dipeptides in search of novel efficient RCS sequestering agents. Eur J Med Chem 2013;66:153-160.
41 Vistoli G, Colzani M, Mazzolari A, Gilardoni E, Rivaletto C, Carini M, Aldini G: Quenching activity of carnosine derivatives towards reactive carbonyl species: Focus on alpha-(methylglyoxal) and beta-(malondialdehyde) dicarbonyls. Biochem Biophys Res Commun 2017;492:487-492.
42 Brings S, Fleming T, De Buhr S, Beijer B, Lindner T, Wischnjow A, Kender Z, Peters V, Kopf S, Haberkorn U, Mier W, Nawroth PP: A scavenger peptide prevents methylglyoxal induced pain in mice. Biochim Biophys Acta 2017;1863:654-662.
43 Mol M, Regazzoni L, Altomare A, Degani G, Carini M, Vistoli G, Aldini G: Enzymatic and non-enzymatic detoxification of 4-hydroxynonenal: Methodological aspects and biological consequences. Free Radic Biol Med 2017;111:328-344.
44 Thornalley PJ: Glyoxalase I--structure, function and a critical role in the enzymatic defence against glycation. Biochem Soc Trans 2003;31:1343-1348.

45 Zemva J, Fleming T, Kaden S, Groene H-J, Schmidt L, Bergheim B, Nawroth P, Tyedmers J: Defense mechanisms against proteotoxic stress triggered by reactive dicarbonyls are up-regulated in diabetic nephropathy: Diabetologia 2016;59:S496-S496.

▶46 Zemva J, Fink CA, Fleming TH, Schmidt L, Loft A, Herzig S, Kniess RA, Mayer M, Bukau B, Nawroth PP, Tyedmers J: Hormesis enables cells to handle accumulating toxic metabolites during increased energy flux. Redox Biol 2017;13:674-686.

▶47 Manda G, Checherita AI, Comanescu MV, Hinescu ME: Redox Signaling in Diabetic Nephropathy: Hypertrophy versus Death Choices in Mesangial Cells and Podocytes. Mediators Inflamm 2015;2015:604208.

▶48 Hipkiss AR: Energy metabolism, proteotoxic stress and age-related dysfunction - protection by carnosine. Mol Aspects Med 2011;32:267-278.

▶49 Babizhayev MA, Lankin VZ, Savel'Yeva EL, Deyev AI, Yegorov YE: Diabetes mellitus: novel insights, analysis and interpretation of pathophysiology and complications management with imidazole-containing peptidomimetic antioxidants. Recent Pat Drug Deliv Formul 2013;7:216-256.

▶50 Velez S, Nair NG, Reddy VP: Transition metal ion binding studies of carnosine and histidine: biologically relevant antioxidants. Colloids Surf B Biointerfaces 2008;66:291-294.

▶51 Mozdzan M, Szemraj J, Rysz J, Nowak D: Antioxidant properties of carnosine re-evaluated with oxidizing systems involving iron and copper ions. Basic Clin Pharmacol Toxicol 2005;96:352-360.

▶52 Decker EA, Livisay SA, Zhou S: A re-evaluation of the antioxidant activity of purified carnosine. Biochemistry (Mosc) 2000;65:766-770.